ANALYTICAL MODEL FOR THIN PLATE DYNAMICS

Joyson Menezes[1], Kadir Kiran[2] and Tony L. Schmitz[1]
[1]Mechanical Engineering and Engineering Science
University of North Carolina at Charlotte
Charlotte, NC, USA
[2]Mechanical Engineering
Suleyman Demirel University
Isparta, Turkey

INTRODUCTION

In many industries, such as aerospace, high-speed milling of flexible components is a common manufacturing process. Productivity in milling thin, monolithic components is often limited by regenerative chatter [1-2]. The present study concentrates on the thin plate dynamics used to model the flexible components. An analytical model is developed for the minimum lateral stiffness of thin ribs with clamped-clamped-clamped-free (CCCF) boundary conditions. The dynamic characteristics of the plate were predicted using finite element analysis and its accuracy was experimentally validated.

The dynamic characteristics of these structures are conventionally described using the complex-valued frequency response function, or FRF, which defines the vibration output to force input ratio in the frequency domain. It represents the steady-state solution to the system differential equation of motion [3, 4].

In this paper, the CCCF plate structure is modeled using finite element software Abaqus/Standard 6.13. The most flexible mode and location in the plate structure are considered when predicting the corresponding stiffness and natural frequency. The analytical model is intended to assist in peripheral milling of flexible structures. The paper is organized as follows. Modeling and identification of the FRF and mode shapes for plates with cantilever (case 1) and CCCF (case 2) boundary conditions using the finite element method, or FEM, are first presented. Next, the experimental procedure is described. Finally, a comparison between predicted and experimental results is presented.

FINITE ELEMENT MODELING

Numerical analysis may be used rather than analytical techniques for complex structures. FEM is the most widely used numerical technique for structural analyses. In FEM the continuum or domain is divided into a series of finite number of regions, called finite elements, which neither overlap nor have a gap between each other. The behavior of each element is controlled by the number of key points on each element called nodes. The displacement or stresses at any point in an element be assigned to these nodes which enables a problem with an infinite number of degrees of freedom to be converted to one with a finite number using differential equations of motion for the nodes. The motion of a dynamic structure or system may be represented by a set of simultaneous differential (coupled) equations using FEM. These coupled equations of motion are solved by transforming them into a set of independent (uncoupled) equations by means of modal matrix. This procedure is called numerical modal analysis [5]. Modal analysis is a process for determining the system's modal parameters, including natural frequency and mode shape. Finite element analysis offers an effective predictive capability for modelling the thin-walled structures.

Analysis procedure

In Abaqus/Standard, modal analysis is referred to as dynamic analysis in which the response of linear systems is calculated on the basis of the necessary modes and frequencies. The procedure for dynamic analysis is summarized as follows.

Natural frequency extraction

Eigenvalue extraction is used to calculate the natural frequencies and the corresponding mode shapes of a system using the Lanczos eigensolver. The eigenvalue problem for natural frequencies of an undamped finite element model is:

$$(-\omega^2 M^{MN} + K^{MN})\,\emptyset^N = 0, \qquad (1)$$

where M^{MN} is the symmetric and positive definite mass matrix; K^{MN} is the stiffness matrix; $\emptyset^N$ is the eigenvector; and M and N are the degrees of freedom [6].

A first step for natural frequency extraction in this study was to build a model with the desired geometric dimensions (Fig. 1) and then assign the material properties and boundary conditions (see Fig. 2). Next, for meshing the model, an eight-node, three dimensional elements with reduced integration (C3D8R) was used. Finer mesh was used for the thin-walled structure (rib) while a coarser mesh was used in the other areas (base). A total of 91908 and 126456 elements were generated for the cantilever and CCCF boundary condition models.

The predicted mode shapes and corresponding natural frequencies for the cantilever and CCCF boundary conditions are shown in Figs. 3-7.

Mode-based steady-state dynamic analysis

After extracting the natural frequencies and mode shapes, the mode-based steady-state dynamic analysis was used to calculate the steady-state dynamic linearized response of each system, i.e., the FRF for harmonic excitation. As the name suggests, this step calculates the response based on the system's eigenfrequencies and modes and, therefore, requires that a natural frequency extraction procedure be performed prior to the steady-state dynamic analysis. The mode-based steady-state dynamic step is defined by specifying the frequency ranges of interest with a linear frequency spacing and a bias parameter of 1. Also, the damping coefficient, i.e., the viscous damping ratio, is defined for a specified mode number and a concentrated nodal force is applied to the displacement degree of freedom at the location of most interest in the structure's response. These loads vary sinusoidally with time over a user-specified range of frequencies [6].

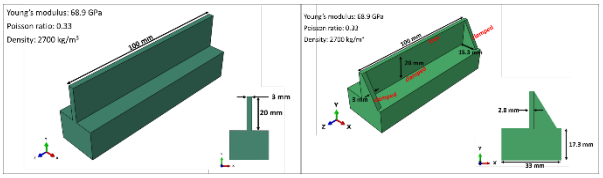

FIGURE 1. A schematic of the monolithic structure with cantilever (left) and CCCF (right) boundary conditions. The inset shows a cross-section of the system and the material properties for 6061-T6 aluminum.

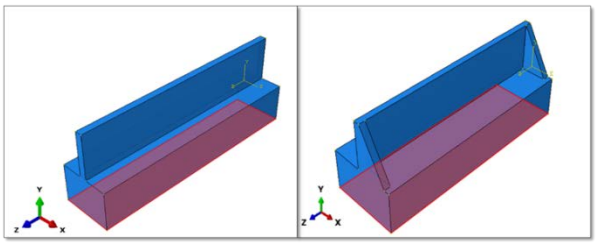

FIGURE 2. FEM encastre boundary conditions for cantilever (left) and clamped-clamped-clamped-free (right) boundary conditions: the bottom face is constrained from all displacements and rotations.

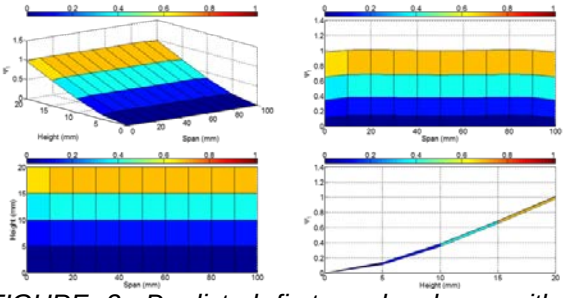

FIGURE 3. Predicted first mode shape with a natural frequency of 5605.2 Hz for cantilever boundary condition.

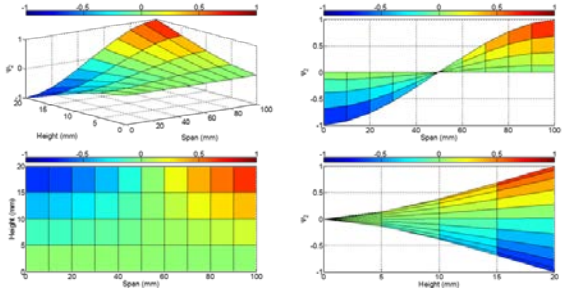

FIGURE 4. Predicted second mode shape with a natural frequency of 6115 Hz for cantilever boundary condition.

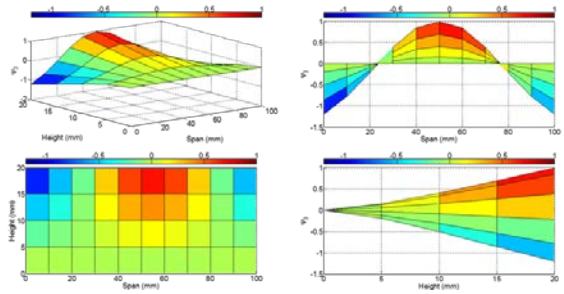

FIGURE 5. Predicted third mode shape with a natural frequency of 7668.5 Hz for cantilever boundary condition.

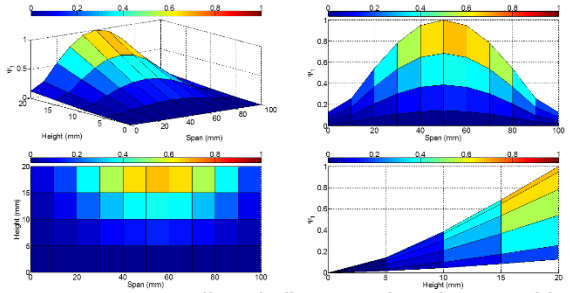

FIGURE 6. Predicted first mode shape with a natural frequency of 5821.9 Hz for CCCF boundary condition.

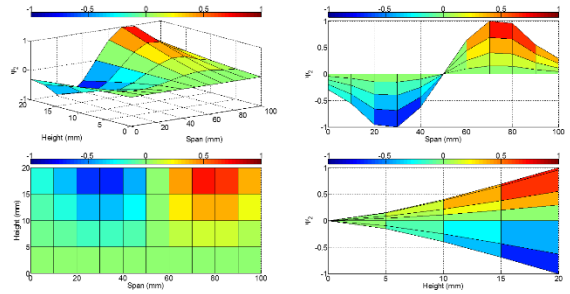

FIGURE 7. Predicted second mode shape with a natural frequency of 7598.1 Hz for CCCF boundary condition.

EXPERIMENTAL SETUP

The plate FRFs were measured using the commercial software package MetalMax. The input force was applied using a modal hammer (PCB 084A17) with a steel tip (PCB 086E80 SN 33416) and the vibration response was measured with a laser vibrometer (Polytec OFV-534); see Figs. 8-9. The vibrometer controller was set for a measurement range of 50 mm/s/V and a 1.5 MHz upper frequency.

In order to obtain FRFs that accurately reflect the predicted workpiece dynamics, it is important to very closely match the workpiece's boundary conditions. Therefore, the workpiece was glued using cyanoacrylate adhesive to a heavy steel table. The laser vibrometer target spot was located at the top right corner of the plate under test with approximately a 295 mm stand-off distance and the structure was impacted with the hammer at multiple locations. Given the time delay between the laser vibrometer and hammer signals, a phase correction algorithm [4] was used to remove the corresponding phase error from the measured FRF.

FEA AND EXPERIMENTAL RESULTS

The predicted and measured mode shapes, stiffness along the free edge, and FRF for cases 1 (cantilever) and 2 (CCCF) are shown in Figs. 10-17.

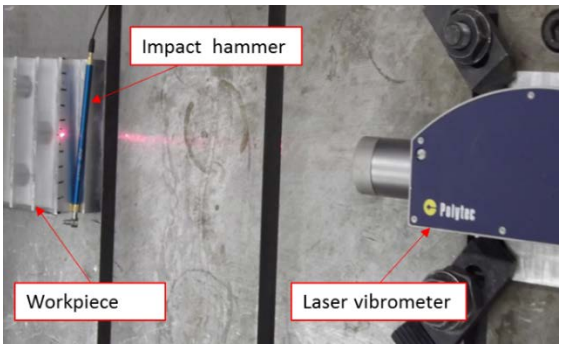

FIGURE 8. Plate with cantilever boundary condition FRF measurement via impact hammer and laser vibrometer.

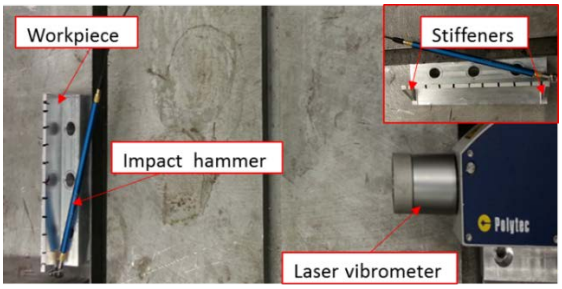

FIGURE 9. Plate with CCCF boundary condition FRF measurement via impact hammer and laser vibrometer. The inset shows stiffeners which provide clamped boundary condition at each end.

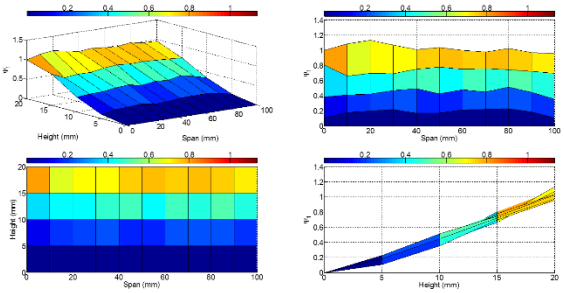

FIGURE 10. Measured first mode shape with a natural frequency of 5774.7 Hz for cantilever boundary condition.

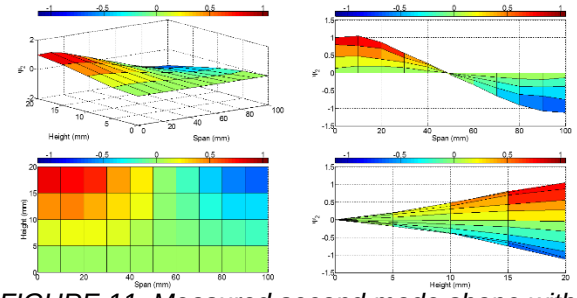

FIGURE 11. Measured second mode shape with a natural frequency of 6319.4 Hz for cantilever boundary condition.

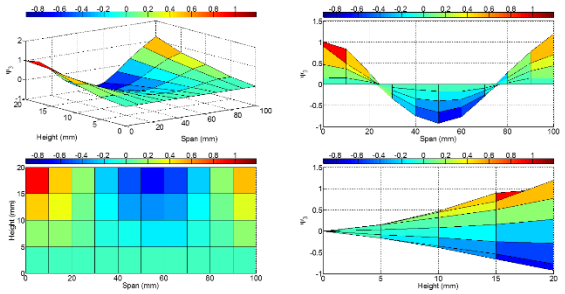

FIGURE 12. Measured third mode shape with a natural frequency of 7939.1 Hz for cantilever boundary condition.

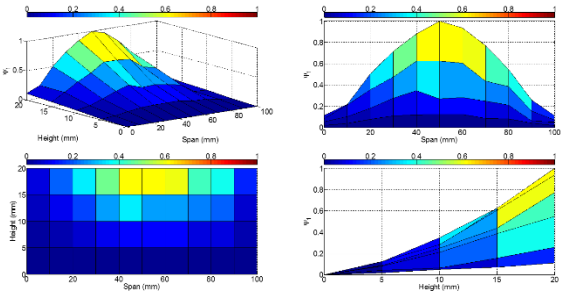

FIGURE 13. Measured first mode shape with a natural frequency of 6002 Hz for CCCF boundary condition.

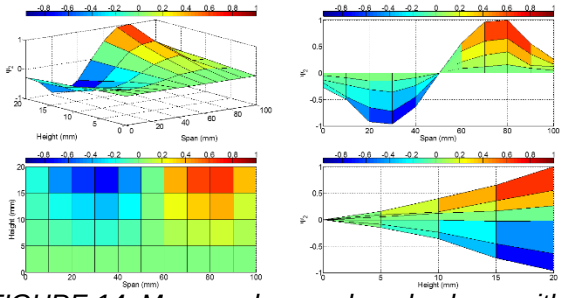

FIGURE 14. Measured second mode shape with a natural frequency of 7795.7 Hz for CCCF boundary condition.

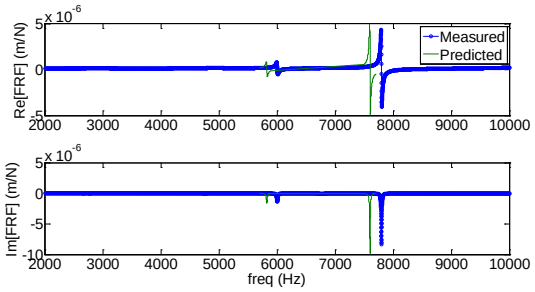

FIGURE 15. Comparison of the predicted and measured FRF for CCCF boundary condition.

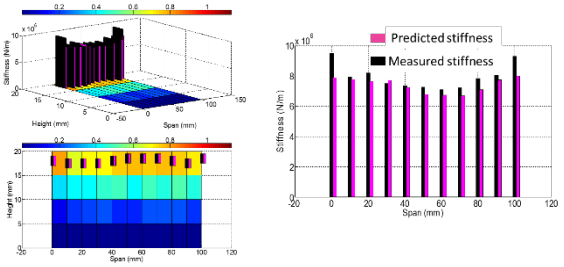

FIGURE 16. Comparison of the predicted and measured first mode stiffness at the free edge for the plate with cantilever boundary condition.

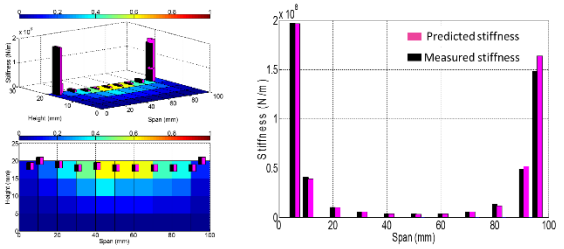

FIGURE 17. Comparison of the predicted and measured first mode stiffness at the free edge for the plate with CCCF boundary condition.

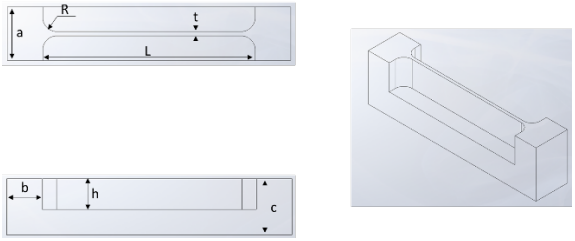

FIGURE 18. Detailed drawing for different test geometries.

TABLE 1. Geometry parameters and material for different test geometries (all dimensions in mm).

Case / Geometry	3	4	5
A	25	25	37.72
B	14.0	13.7	24.76

c	36.91	47.86	53.75
R	11.43	11.43	10
L	150	150	150
t	2.01	2.01	2.95
h	30	40	30
Material	Al6061	Al6061	Ti6Al4V

Further analyses were conducted on other plate geometries with CCCF boundary conditions. Natural frequencies are shown in Fig. 19 and Table 1.

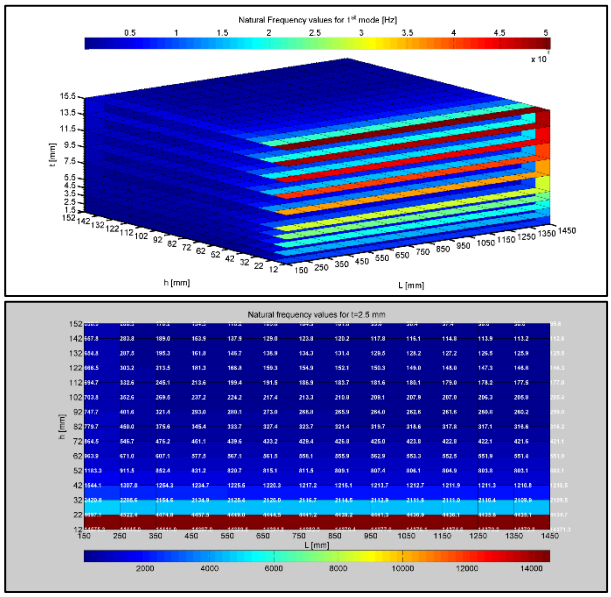

FIGURE 19. Natural frequency values for (top) entire range (bottom) 2.5 mm thickness only.

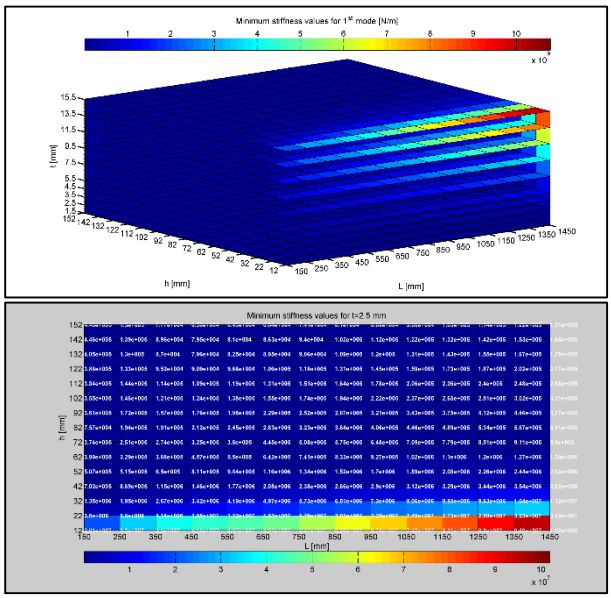

FIGURE 20: Minimum stifness values for (top) entire range (bottom) 2.5 mm thickness

Finally, using the numerical FEA modeling capability, the minimum stiffness and its corresponding natural frequency (for first mode) was evaluated for changes in length ranging from 150 to 1450 mm, thickness from 1.5 to 15.5 mm, and height from 12 to 152 mm. The result is shown in Fig. 20. All results are summarized in Table 2.

TABLE 2. Comparing the first mode predicted and measured modal parameters for different test geometries.

Test geometry / Modal Parameters	Case 1	Case 2	Case 3	Case 4	Case 5
Measured natural frequency, f_{n_m}(Hz)	5757.9	5994.4	2238.5	1468.7	3123.5
Predicted natural frequency, f_{n_p} (Hz)	5605.7	5822.1	2173.4	1415.2	3100.3
$(f_{n_m} - f_{n_p})/f_{n_m}$ x 100 (%)	2.7	2.9	2.9	3.6	0.74
Measured modal stiffness, k_m (N/m) (x 10^6)	7.2581	3.721	0.5311	0.302	2.6382
Predicted modal stiffness, k_p (N/m) (x 10^6)	6.7672	3.406	0.5514	0.2904	2.5451
$(k_m - k_p)/k_m$ x 100 (%)	6.8	8. 5	-3.8	3.8	3.5

CONCLUSIONS

In this study, a comparison of predicted and measured natural frequencies, stiffness values, and mode shapes showed good agreement for thin-walled structures with cantilever and clamped-clamped-clamped-free boundary conditions. Using the numerical finite element modeling capability, the natural frequency and minimum stiffness for the first (most flexible) mode was evaluated over a range of lengths, thicknesses, and heights. These trends may then combined into a lookup table that can be used to identify the natural frequency and minimum rib stiffness for the selected geometry. Using the interpolated natural frequency and

stiffness values, the workpiece dynamics can be defined and, using milling stability analysis methods, stable machining parameters may be identified.

REFERENCES

[1] Sèbastian Seguy, Gilles Dessein, Lionel Arnaud, Surface roughness variation of thin wall milling, related to modal interactions, International Journal of Machine Tools and Manufacture 48 (2008) 261-274.

[2] Scott Smith, Robert Wilhelm, Brian Dutterer, Harish Cherukuri, Gaurav Goel, Sacrificial structure preforms for thin part machining, Annals CIRP 61 (2012) 379-382.

[3] T. Schmitz, S. Smith, Mechanical Vibrations: Modelling and Measurements, Springer, New York, NY, 2012.

[4] V. Ganguly, T. Schmitz, Phase correction for frequency response function measurements, Precision Engineering 38 (2014) 409-413.

[5] Zu-Qing Qu, Model Order Reduction Techniques with Applications in Finite Element Analysis, Springer Science and Business Media, 2013.

[6] Dassault Systemes Simulation Corp., User's Manual Version 6.13-2, Providence, RI, 2013.